Density of states and Wannier-Stark levels of superlattices in an electric field

M. Ritze
Institute of Theoretical Physics, Department of Physics, Humboldt University, Invalidenstrasse 110, O-1040 Berlin, Germany

N. J. M. Horing
Department of Physics and Engineering Physics, Stevens Institute of Technology, Hoboken, New Jersey 07030

R. Enderlein
Institute of Theoretical Physics, Department of Physics, Humboldt University, Invalidenstrasse 110, O-1040 Berlin, Germany
(Received 12 November 1992)

The density of states is calculated for superlattices in the presence of an electric field, using the concept of a generalized transmission probability. Various $Ga_{1-x}Al_xAs$-based quantum-well structures with up to 200 periods are examined for electric fields ranging from 4×10^2 V/cm to 1×10^6 V/cm. Different field effects are observed in the below- and above-barrier regions of the density-of-states spectra. In the below-barrier region the spectra embody the occurrence of Wannier-Stark localization. The above-barrier region is dominated by two kinds of structures, one similar to Franz-Keldysh oscillations, and another resembling a Wannier-Stark-ladder behavior.

I. INTRODUCTION

The effect of an external electric field on the electronic properties of single (SQW) and multiple (MQW) quantum wells, as well as superlattices (SL's) has attracted much attention in recent years.[1–23] In optical measurements like electroabsorption,[18] electroreflectance,[19] or photoreflectance,[20] one observes Franz-Keldysh oscillations,[24,25] Stark shifts, and Wannier-Stark (WS) ladders.[26] The WS ladders are also seen in luminescence and photoconductivity.[9,22] Time-resolved optical[23] experiments give evidence for Bloch oscillations in SL minibands, the time-domain equivalent of the Stark ladder which, similar to the Stark ladder itself, has never been observed in bulk materials.

Various theoretical techniques have been applied in order to understand the electric-field effects on quantum well (QW) and SL structures, e.g., perturbation theory, variational calculations of quasistationary energy levels,[1] transmission probability studies,[3] and investigations of the density of states (DOS).[2,10,21] The definition of the DOS for systems in an electric field as well as other systems having continuous-energy spectra represents a problem on its own. It may be solved in different ways. If a finite transmission probability exists for a plane-wave state penetrating from $-\infty$ to ∞, this probability may be taken to be representative for the DOS. If no such probability exists one may use a generalization of the transmission probability expression which exists also under more general circumstances, or one may consider the change of the DOS due to a finite potential instead of the DOS itself. The latter procedure has been applied to heterostructures in an electric field by Austin and Jaros[2] and, in a slightly different version, by Trezeciakowski and Gurioli.[21] In the present paper we will deal with the DOS. Since no transmission probability exists in the presence of a homogeneous electric field, it becomes necessary to use the generalized DOS expression from Ref. 27. So far it has been utilized only for SQW's.[10] Here we will apply it to SL structures for the first time. Our aim is, in particular, to demonstrate how Stark ladders or Bloch oscillations manifest themselves in the DOS. In Sec. II we specify the generalized DOS expression to MQW's and SL's by using transfer matrices. We also demonstrate that the generalized DOS turns into the transmission probability if the latter exists. In calculating the DOS of MQW's and SL's in an electric field we distinguish between energies below and above the barriers. The below-barrier region is treated in Sec. III A, and the above-barrier region in Sec. III B.

II. DENSITY OF STATES

A. Generalized DOS expression

It has been demonstrated[27] that the DOS $\rho(E)$ per unit energy and lengths for an electron in a one-dimensional system having a continuous energy spectrum may be defined as

$$\rho(E)=\left[\int_{-\infty}^{\infty}dE'\int_{-\infty}^{\infty}dx\,\varphi_{E'}^{\mathrm{EQW}*}(x)\varphi_E^{\mathrm{EQW}}(x)\right]^{-1}. \quad (1)$$

Here $\varphi_E^{\mathrm{EQW}}(x)$ refers to eigensolutions of the Schrödinger equation

$$\left[\frac{p^2}{2m^*}+V(x)\right]\varphi_E^{\mathrm{EQW}}(x)=E\varphi_E^{\mathrm{EQW}}(x), \quad (2)$$

normalized such that they possess equal quantum weights (EQW's). In Eq. (2) m^* means the effective mass and $V(x)$ the potential of an electron. The EQW normalization is introduced as follows: The potential $V(x)$ is decomposed in a part $V_{\mathrm{fin}}(x)$ having finite values at $-\infty$ and at ∞, and a remaining part $V_0(x)$, so that

$V(x)=V_{\text{fin}}(x)+V_0(x)$ holds. Then the EQW normalized solutions $\varphi_E^{\text{EQW}}(x)$ are defined by the asymptotic condition

$$\varphi_E^{\text{EQW}}(x)=\varphi_E^{0,\text{EQW}}(x), \quad x\to\infty , \tag{3}$$

with $\varphi_E^{0,\text{EQW}}(x)$ being the EQW normalized solution of the homogeneous Schrödinger equation

$$\left[\frac{p^2}{2m^*}+V_0(x)\right]\varphi_E^{0,\text{EQW}}(x)=E\varphi_E^{0,\text{EQW}}(x) . \tag{4}$$

The EQW normalization of the homogeneous solution $\varphi_E^{0,\text{EQW}}(x)$ means that expression (1) results in the correct DOS $\rho^0(E)$ of the homogeneous system if $\varphi_E^{\text{EQW}}(x)$ is replaced with $\varphi_E^{0,\text{EQW}}(x)$. Here $\rho^0(E)$ is thought to be known already from other calculations. If, for instance, $V_0(x)=0$, then one knows that $\rho^0(E)=(1/2\pi)\sqrt{2m^*/(\hbar^2E)}$.

The normalization integral in (1) may be taken by means of the Green's formula and Schrödinger's equation (2). One obtains

$$\int_{-\infty}^{\infty} dx\, \varphi_{E'}^{\text{EQW}*}(x)\varphi_E^{\text{EQW}}(x)=\frac{\hbar^2}{2m^*}\frac{[\varphi_{E'}^{\text{EQW}*}(x)\varphi_E'^{\text{EQW}}(x)-\varphi_{E'}'^{\text{EQW}*}(x)\varphi_E^{\text{EQW}}(x)]_{-\infty}^{\infty}}{E'-E} . \tag{5}$$

In order to make the DOS definition (1) still more transparent we demonstrate that it reduces to the transmission probability if this probability exists.

B. Relation to transmission probability

In order to allow for a nonzero transmission probability between $x=-\infty$ and $x=\infty$, the potential $V(x)$ must remain finite at infinity. For simplicity, we assume that $V(-\infty)=V(\infty)=0$ holds. Then $V_{\text{fin}}(x)=V(x)$ and $V_0(x)=0$. The homogeneous Schrödinger equation (4) turns into that of a free particle. The corresponding EQW solutions are plane waves e^{ikx} with $E=E(k)=(\hbar^2k^2/2m^*)$.[27] Thus the EQW solutions of the full Schrödinger equation (2) follows by means of the asymptotic condition

$$\varphi_E^{\text{EQW}}(x)=e^{ikx}, \quad x\to\infty . \tag{6}$$

Owing to relation (5) the orthonormality integral depends only on the asymptotic values of $\varphi_E^{\text{EQW}}(x)$ for $x\to-\infty$ and $x\to\infty$. For $x\to-\infty$ one has

$$\varphi_E^{\text{EQW}}(x)=a(E)e^{ikx}+b(E)e^{-ikx}, \quad x\to-\infty . \tag{7}$$

Here $a(E)$ and $b(E)$ are coefficients which follow from the Schrödinger equation (2). The continuity of the probability flow stated by this equation means that

$$|a(E)|^2=1+|b(E)|^2 . \tag{8}$$

By using relations (5), (6), and (7), the orthonormality integral becomes

$$\int_{-\infty}^{\infty} dx\, \varphi_{E'}^{\text{EQW}*}(x)\varphi_E^{\text{EQW}}(x)=\pi[1+|a(E)|^2+|b(E)|^2]\delta(k-k') . \tag{9}$$

The DOS according to formula (1) reads

$$\rho(E)=\frac{1}{2\pi}\frac{1}{|a(E)|^2}\left[\frac{dE}{dk}\right]^{-1} . \tag{10}$$

Here $1/|a(E)|^2$ represents the ratio of the transmitted and incoming probability flows, i.e., the transmission coefficient $T(E)$. Thus one may also write

$$\rho(E)=\frac{1}{2\pi}T(E)\left[\frac{dE}{dk}\right]^{-1} . \tag{11}$$

This means that under the conditions specified above, the DOS per unit energy and length given by expression (1) represents nothing but the transmission coefficient $T(E)$, multiplied with the Wronskian factor of the $E(k)$ transformation.

C. Application to heterostructures in an electric field

We consider planar heterostructures with N wells and $N-1$ barriers, embedded within two barrier layers extending infinitely, as shown in Fig. 1. The layers of the entire structure, including the embedding barrier layers, are numbered consecutively by an index i beginning with $-N$ for the embedding barrier on the left side. The interface positions are denoted by x_i, where the index i refers to the layer on the right side of the interface. The zero-field potential in each layer is denoted by V_i, where V_i equals V in a barrier and 0 in a well (see Fig. 1). The zero point of energy is at the bottom and the one of the x axis is at the center of the rightmost QW. For simplicity, the effective electron masses are taken to be the same in the well and barrier materials.

Then the Schrödinger equation (2) in layer i of the structure has the form

$$\left[-\frac{\hbar^2}{2m^*}\frac{d^2}{dx^2}+eFx+V_i\right]\varphi_E^{\text{EQW}}(x)=E\varphi_E^{\text{EQW}}(x) \tag{12}$$

for x in layer i.

To facilitate solution, we set

$$z=-\left[\frac{2m^*}{(\hbar eF)^2}\right]^{1/3}[E-eFx-V(x)] \tag{13}$$

where

$$\frac{d^2}{dz^2}\varphi_E^{\text{EQW}}(z)-z\varphi_E^{\text{EQW}}(z)=0 . \tag{14}$$

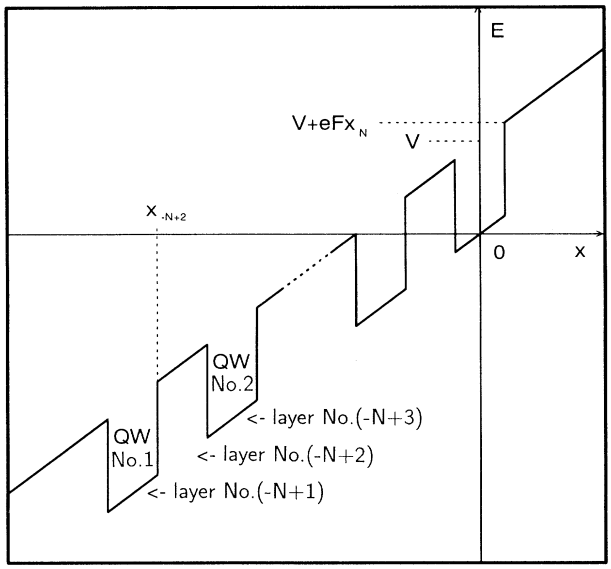

FIG. 1. Potential profile of a QW structure consisting of N QW's with well thickness d_W, barrier thickness d_B, and height V in an electric field F.

The general solution of this equation is given in terms of the Airy functions $Ai(z)$ and $Bi(z)$.[28] For x in layer i one has

$$\varphi_E^{\mathrm{EQW}}(x)=a_i\,Ai\left[\frac{eFx+V_i-E}{\hbar\theta}\right]+b_i\,Bi\left[\frac{eFx+V_i-E}{\hbar\theta}\right], \tag{15}$$

with

$$\theta=[(eF)^2/(2m^*\hbar)]^{1/3} \tag{16}$$

being the electro-optical frequency. The determination of the coefficients a_i and b_i is carried out using the standard quantum-mechanical matching conditions at the interfaces. Employing Eq. (15) they can be written as

$$M_i^{i-1}\begin{bmatrix}a_{i-1}\\ b_{i-1}\end{bmatrix}=M_i^i\begin{bmatrix}a_i\\ b_i\end{bmatrix}, \tag{17}$$

where

$$M_i^j=\begin{bmatrix} Ai\left[\frac{eFx_i+V_j-E}{\hbar\theta}\right] & Bi\left[\frac{eFx_i+V_j-E}{\hbar\theta}\right] \\ Ai'\left[\frac{eFx_i+V_j-E}{\hbar\theta}\right] & Bi'\left[\frac{eFx_i+V_j-E}{\hbar\theta}\right]\end{bmatrix} \tag{18}$$

and $Ai'=dAi(x)/dx$, etc. A transfer-matrix representation follows as

$$\begin{bmatrix}a_{i-1}\\ b_{i-1}\end{bmatrix}=T_{i-1,i}\begin{bmatrix}a_i\\ b_i\end{bmatrix}, \tag{19}$$

with the transfer matrix $T_{i-1,i}$ given by

$$T_{i-1,i}=(M_i^{i-1})^{-1}M_i^i . \tag{20}$$

The initial values a_N and b_N of the coefficients a_i and b_i are obtained by means of the asymptotic condition (3). The homogeneous EQW solutions $\varphi_E^{0,\mathrm{EQW}}$ read here[27]

$$\varphi_E^{0,\mathrm{EQW}}(x)=Ai\left[\frac{eFx+V_i-E}{\hbar\theta}\right] \tag{21}$$

for x layer i. Thus condition (3) yields

$$a_N=1 \quad \text{and} \quad b_N=0 . \tag{22}$$

All other coefficients a_i and b_i $(-N\le i<N)$ can be calculated by applying the transfer matrix given in Eq. (20).

Once the wave function $\varphi_E(x)$ is known, the determination of the DOS $\rho(E)$ calls for the evaluation of the normalization integral (5). Utilizing Eq. (15) we find

$$\rho(E)=(a_{-N}^2+b_{-N}^2)^{-1}\rho_0 ,\qquad \rho_0=\left[eF\left[\frac{\hbar^2}{2m^*}\right]^2\right]^{-1/3} . \tag{23}$$

Here ρ_0 represents the DOS in a homogeneous electric field without the SL.

III. RESULTS

SL structures consisting of GaAs wells and $Ga_{1-x}Al_xAs$ barriers are considered. The electron mass m^* equals $0.0665m_0$. The structures to be examined here are listed in Table I. The zero-field energy spectra have different character in the energy regions below and above the barriers. They are discrete below the barriers, and continuous above them. This results in different field effects in these two regions.

TABLE I. Parameters of the structures examined.

Name	No. of QW's	d_W (Å)	d_B (Å)	V (eV)
SQW1	1	51		0.2
SQW2	1	51		0.366
SL1	5	51	51	0.2
SL2	10	51	23	0.2
SL3	10	51	51	0.2
SL4	10	51	102	0.2
SL5	10	74	40	0.366
SL6	10	51	23	0.366
SL7	50	51	51	0.2
SL8	200	51	51	0.2

A. Below-barrier region

1. Structures with one band below the barrier

The DOS of SQW1 in the presence of a weak electric field is displayed in Fig. 2(a). It exhibits only one peak at an energy of 0.074 eV. This energy equals to the energy of the corresponding zero-field bound state. Figures 2(b)–2(d) show the DOS of DQW structures consisting of two SQW1's separated by a barrier of varying width. For a barrier width d_B of 102 Å [Fig. 2(b)] the higher energetic peak indicates a level at 0.074 eV which, again, coincides with the SQW1 peak. The other peak is less than 1 meV below this, differing only very slightly from the expected WS separation [$\Delta_F = eF(d_W + d_B)$]. A decrease of the barrier width, as in Figs. 2(c) and 2(d), results in an obvious change of the peak positions and an increase of their separation Δ. Here the two peaks are found in almost symmetric positions with respect to the SQW peak. Their separation is much greater than the WS separation Δ_F. Analogous results are obtained for structures with more QW's. Figure 3 depicts parts of the DOS spectra of SL3. For not-too-high fields, a series of pronounced peaks occurs below V_N. The number of these peaks equals the number of wells. They again correspond to the zero-field bound states, forming the energy bands in the case of SL's. In addition, there are less-pronounced peaks in Fig. 3 which are due to above-barrier states. We discuss them at the end of this section. In the case of thick barriers the positions of the pronounced peaks shift linearly with F in the whole range of field strengths [Fig. 4(a)]. For thinner barriers the F dependence of these peaks becomes sublinear in the low-field range [Fig. 4(b)], and remains linear in the high-field range [Fig. 4(c)]. In general, the positions of the pronounced peaks may be

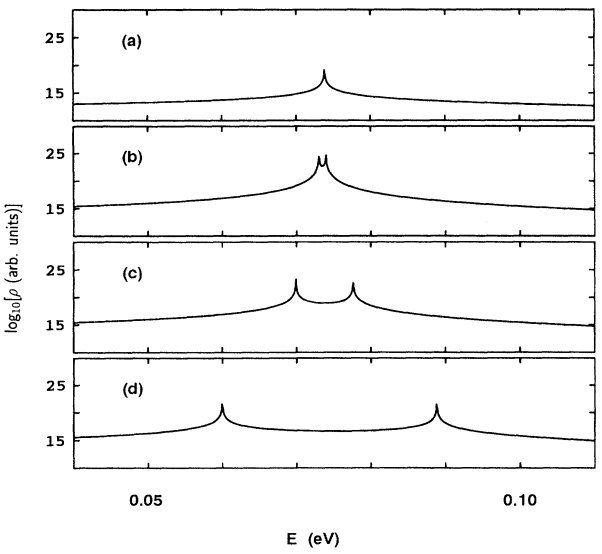

FIG. 2. DOS of (a) SQW1 and DQW's with (b) $d_B = 102$ Å, (c) $d_B = 51$ Å, (d) $d_B = 23$ Å. $F = 4 \times 10^2$ V/cm, $d_W = 51$ Å, $V = 0.2$ eV.

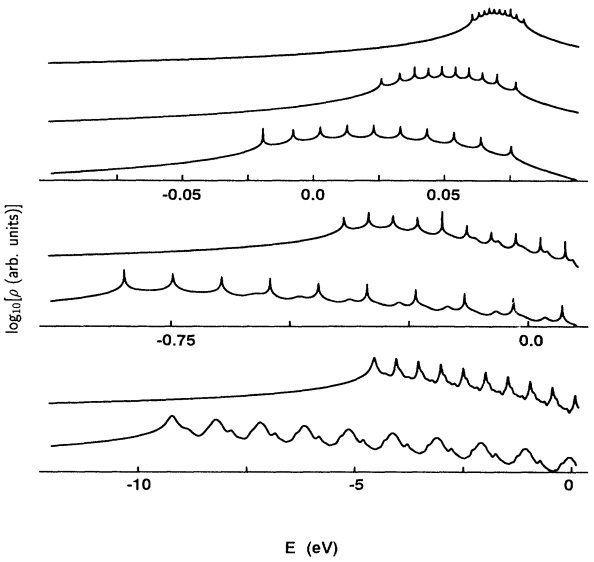

FIG. 3. DOS of SL3.

understood as the result of the interplay between the two interactions involved, that between different QW's, and that with the electric field. For low enough fields the first dominates, and for sufficiently strong the second. This may also be seen from Fig. 5, where the averages of the peak separations versus field are plotted for different barrier widths. For strong enough fields the levels may be understood as broadened WS levels, the broadening energy being given by $\hbar\theta$, with θ from Eq. (16). This interpretation follows from the localization behavior of wave functions with energies at peak positions (Fig. 6). For weak fields the wave functions are delocalized [Figs. 6(a) and 6(b)], and the states form bands, i.e., they are *band levels.* An increase of the field causes the localization in a certain QW [Fig. 6(c)] and transforms the band levels continuously into WS levels. The transition occurs if the level separation reaches about twice the zero-field separa-

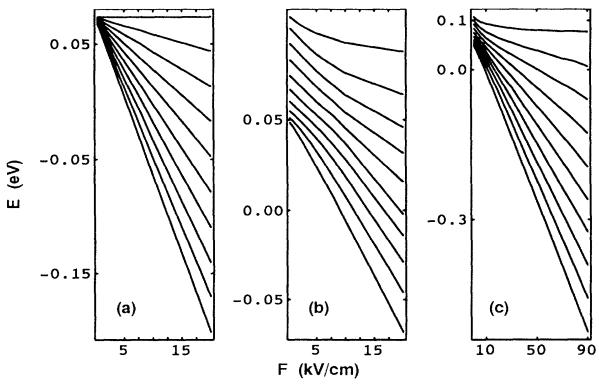

FIG. 4. Energies of pronounced DOS peaks vs F for (a) SL4 and (b) and (c) SL2.

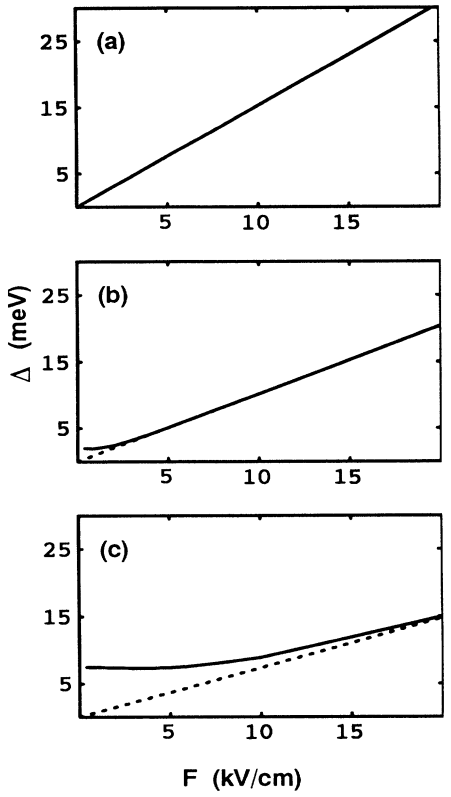

FIG. 5. Average peak separation Δ vs F for (a) SL4, (b) SL3, and (c) SL2 [dashed line, $\Delta_F = eF(d_W + d_B)$].

tion. This is appreciably less than the zero-field bandwidth, which often has been used as measure. Furthermore, the shape of the DOS peaks changes, as can be seen in Fig. 3. With increasing field the peaks become broader and broader. For very high fields $F \geq 10^6 - 10^7$ V/cm the clear WS periodicity vanishes. This is due to the onset of tunneling through the barrier if $\hbar\theta$ becoming greater than V (see Fig. 7), which causes the localization and the corresponding WS ladder to disappear.

Figure 3 reveals that the spacing between the peaks at either edge of the band is smaller than the spacing of central peaks. This difference follows from their different localizations: the outer peaks belong to states localized in the outer QW's, and the central peaks to states in the central QW's. Hence, the outer peaks originate from states that lack the interaction with other states on their respective continuum sides. The low-field energetic difference of the energetically lowest and highest states is a measure of the (zero-field) bandwidth. Our calculations yield a bandwidth of 0.6 meV for SL4 and 59 meV for SL2.

The so-called "above-barrier" states[4] have been neglected so far. This term refers to states with energies between $V_{-N} + eFx_{-N+1}$ and $V_N + eFx_N$ that produce DOS peaks, but do not correspond to zero-field bound states. A comparison of Figs. 8(a) and 8(b) reveals the nature of such "above-barrier" states. Figure 8(a) depicts the squared wave function of a WS state confined to the seventh QW: its energy is -0.266 eV and the level lies inside the QW. The "above-barrier" state that belongs to the same QW depicted in Fig. 8(b) is localized in the barrier layers surrounding the seventh QW. Clearly, its localization is not as complete as that of the WS state. The

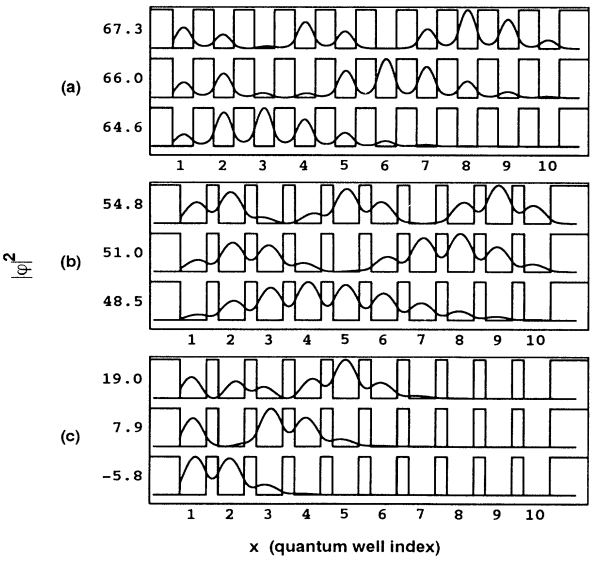

FIG. 6. $|\varphi|^2$ vs x for (a) SL4, $F = 0.5$ kV/cm, (b) SL2, $F = 0.5$ kV/cm, and (c) SL2, $F = 10$ kV/cm. Peak energies are given in meV.

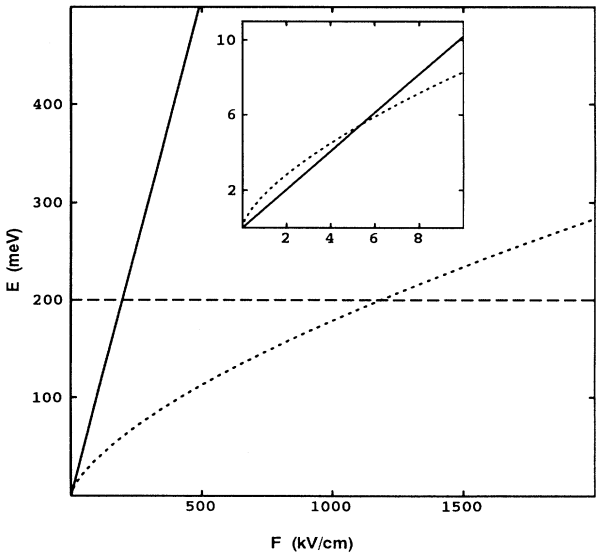

FIG. 7. Field dependence of characteristic energies for a structure with $N \geq 5$, $d_W = d_B = 51$ Å, and $V = 200$ meV. The dashed line indicates V, the dotted line $\hbar\theta$, whereas the solid line represents eFd. The inset shows the magnified lower left part of the drawing.

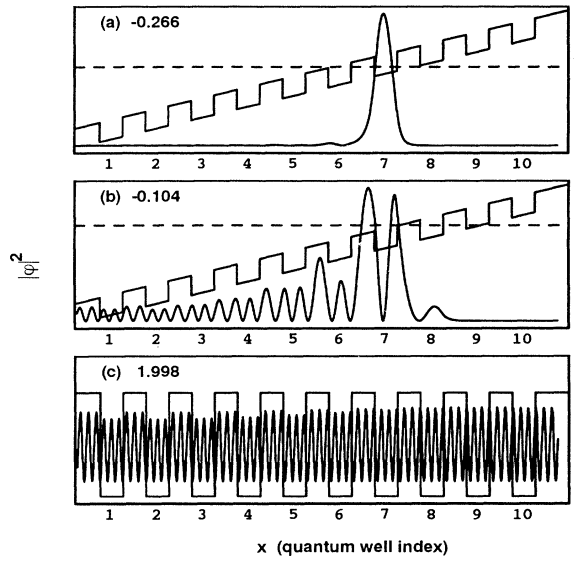

FIG. 8. Localization of (a) a WS state (SL3, $F=1.1\times10^5$ V/cm), (b) an "above-barrier" state (SL3, $F=1.1\times10^5$ V/cm), and (c) a state corresponding to a "short-period" oscillation peak (SL3, $F=3\times10^4$ V/cm) in terms of $|\varphi|^2$ vs x. The dashed line indicates the energy of the state.

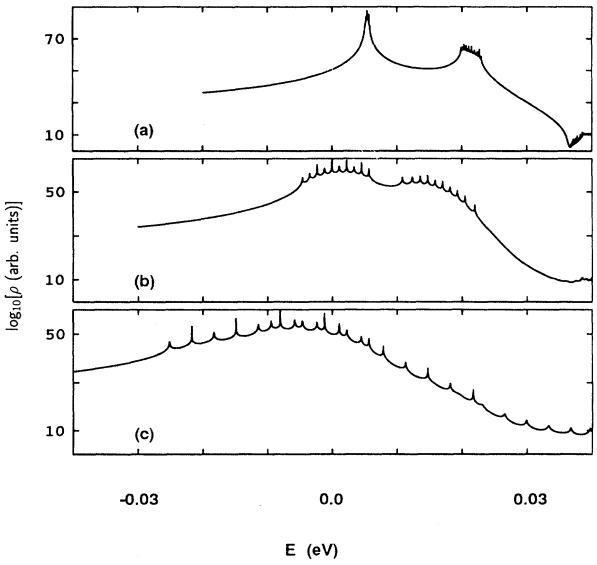

FIG. 9. DOS of SL5 (a) for $F=4\times10^2$ V/cm, (b) for $F=1\times10^4$ V/cm, (c) for $F=3\times10^4$ V/cm.

energy of this "above-barrier" state is -0.104 eV, and as can be seen in Fig. 8(b), this energy lies above the seventh QW. Obviously, the "above-barrier" states are pushed downward out of the continuum above V_N+eFx_N. For higher fields, more of these states occur. The "above-barrier" peaks in the DOS are wider and not as pronounced as WS peaks, because the confinement of the corresponding wave function is weaker.

So far, results were presented for SL's with ten or fewer QW's. In experiment, SL's with larger numbers of QW's are frequently used. Of course, these structures generally have the same properties as smaller ones (WS ladder, level separation, localization, etc.). Investigations of SL's with 50, 100, or even 1000 QW's in low and moderate electric fields reveal that the splittings of the two–five outermost Stark levels can differ from the splittings of the other levels. This is due to the finiteness of the SL structure, i.e., the missing periodicity. It is a further hint on the localization of the electronic states. Since Stark levels that are separated equidistantly do not feel the impact of the external barriers, the wave functions can extend over 5–11 QW's.

2. *Structures with more than one band below the barrier*

SL structures composed of QW's with more than one zero-field bound level below the barrier are investigated in this section. In general, the effects described in the previous sections occur in these structures as well, and we will focus here on new properties.

The low-field DOS of SL5 is shown in Fig. 9(a). It exhibits two bands below the barriers. The different spacings between the WS levels of the two bands follow from their different bandwidths for zero field, where a higher band is wider than a lower one. The electric field pushes the WS peaks towards lower energies, except that the energetically highest peak of each band remains almost unaltered [Figs. 9(b) and 9(c)]. With increasing field, the WS ladder spacings of both bands approach Δ_F. Thus, a rising field causes the higher band to approach the lower one. When the bands cross, the DOS peaks are lowered and broadened considerably. This indicates the onset of resonant tunneling between the upper and lower band states, i.e., interband tunneling occurs.

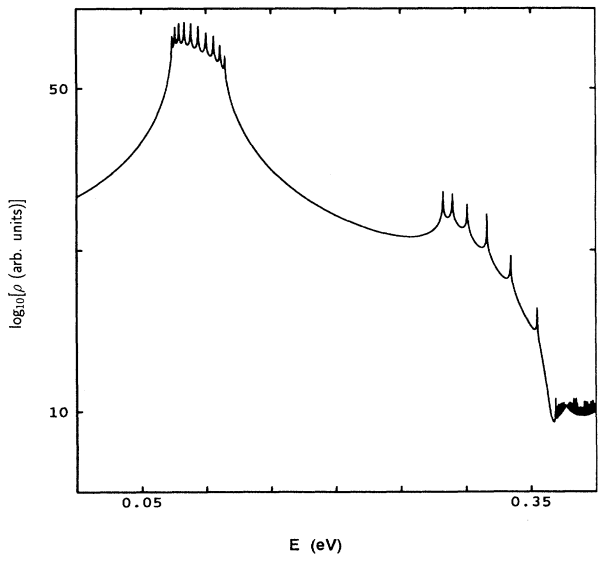

FIG. 10. DOS of SL6 for $F=1\times10^3$ V/cm.

The large bandwidth of a SL may result in an incomplete Stark ladder for bands close to the barrier potential V. An example of an incomplete Stark ladder is depicted in Fig. 10. Only the six lowest levels have an energy less than the corresponding value of $V_{2i-N}+eFx_{2i-N}$. The remaining four states are pushed upward into the continuum above V_N+eFx_N.

B. Above-barrier region

1. Analytic results

Assuming low fields and a small number (1,2, . . .) of QW's, the coefficients a_{-N} and b_{-N} governing the DOS in (23) may be determined analytically by means of the asymptotic expansions of the Airy functions.[28] Considering only the leading terms, one obtains expressions for a_{-N} and b_{-N} of the general form

$$a_{-N},b_{-N}\approx \sum c \left[f_1(\delta_{-N+1})f_2(\delta_N) \times \prod_i g_i(\gamma_i-\gamma_{i+1}) \times \prod_j h_j(\delta_j-\delta_{j+1}) \right], \quad (24)$$

where i runs over all well layers ($i=-N+1,-N+3,\ldots,N-1$), and j over barrier layers ($j=-N+2,-N+4,\ldots,N-2$). Furthermore,

$$\gamma_i=\tfrac{2}{3}\alpha_i^{3/2}+\frac{\pi}{4},\quad \alpha_i=\frac{E-eFx_i}{\hbar\theta}, \quad (25)$$

$$\delta_j=\tfrac{2}{3}\beta_j^{3/2}+\frac{\pi}{4},\quad \beta_j=\frac{E-V-eFx_j}{\hbar\theta}, \quad (26)$$

and each of the functions f_1, f_2, g_i and h_j stands for a sin or cos function. The coefficients c are products of $\alpha_i^{\pm 1/4}$ and $\beta_i^{\pm 1/4}$, with the sum of the powers equaling zero. The number of terms to be summed up in (24) depends on the number of QW's in the SL. For a SQW, the sum has four terms; in the case of a DQW there are already 128 terms. These analytic results will be useful for the interpretation of the numerical DOS spectra below.

2. Numerical results

The zero-field DOS spectrum is continuous for energies above V_N. For an infinite SL one gets a band structure with clear gaps. Since only finite numbers of QW's are considered here, the gaps are incompletely manifested depending on the actual number of quantum wells. As shown in Figs. 11(a) and 11(b), an increase of the QW number results in more-pronounced gaps. However, a structure with five QW's (SL1) has its gaps already at the same positions as structures with many more QW's (see Fig. 12). Imposing an electric field on the structure has to be considered as a disturbance of the regular order of the quantum wells, reducing the wave function overlap and, thus, affecting the formation of gaps. Nevertheless,

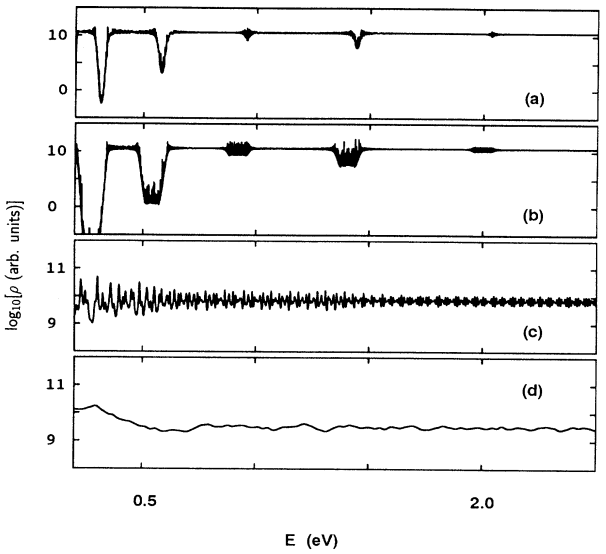

FIG. 11. DOS of (a) SL7 for $F=5\times10^2$ V/cm, (b) SL8 for $F=5\times10^2$ V/cm, (c) SL7 for $F=8\times10^4$ V/cm, (d) SL7 for $F=5\times10^5$ V/cm.

the band structure is still visible for low fields ($F<10^4$ V/cm) [Fig. 11(a)]. Increasing the field above 10^4 V/cm results in the vanishing of gaps [Fig. 11(c)].

A close look at the low-field DOS [Figs. 12(a) and 12(b)] shows that its most striking feature is a kind of oscillation manifesting itself as a modulation of the dark areas. Figure 12(c) exhibits these "long-period" oscillations revealing that they consist of "short-period" oscillations. The latter ones are described analytically by the functions f_1 and f_2 in expression (24). For the positions

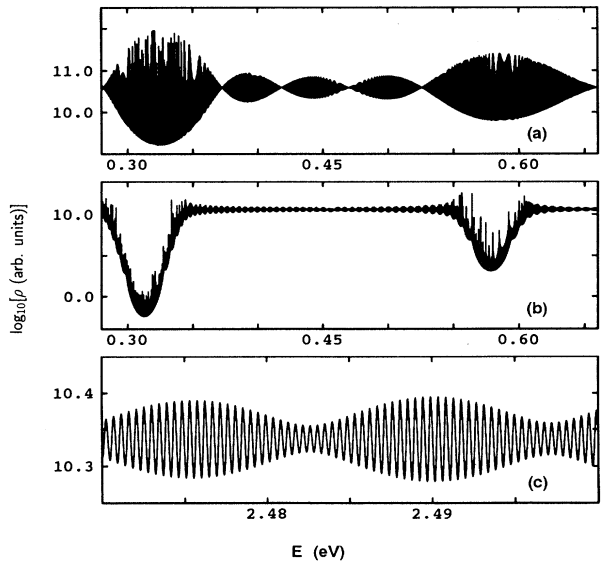

FIG. 12. DOS of (a) SL1, (b) SL7, both for $F=5\times10^2$ V/cm, and (c) SL7 for $F=3\times10^3$ V/cm.

E_n^s of the nth peak, one obtains from (26) in lowest approximation with respect to F

$$E_n^s \approx [\tfrac{3}{2}\pi(n-\tfrac{1}{4})]^{2/3}\hbar\theta + V \ . \tag{27}$$

The proportionality of E_n^s with θ indicates a similarity of these oscillations to the well-known Franz-Keldysh oscillations. The corresponding periods Δ_n^s at large n are approximately

$$\Delta_n^s = \pi \frac{\hbar eF}{\sqrt{2m^* E_n^s}} \ . \tag{28}$$

Surprisingly, they are linear in the electric field, although they have nothing in common with the WS levels. The linear dependency of Δ_n^s on F is also found in the numerical results. For $F = 5\times 10^2$ V/cm and $E = 2.5$ eV one has $\Delta^s = 0.075$ meV, which agrees very well with the value of 0.076 meV obtained from the calculated DOS spectra. The lowest-order approximation in Eq. (28) breaks down for $F \geq 3\times 10^4$ V/cm. For higher fields ($F \geq 8\times 10^4$ V/cm) one "long-period" oscillation consists only of a few "short-period" oscillations.

An inspection of the "long-period" oscillations in Fig. 12 shows that all bands have the same number of them, the number being given by the number of SL periods. This observation indicates a similarity between the "long-period" peaks and the band or WS levels below the barriers. Analytically, the "long-period" oscillations are described by the functions g_i and h_j in (24). As their respective arguments $(\gamma_i - \gamma_{i+1})$ and $(\delta_j - \delta_{j+1})$ indicate, these oscillations emerge from interferences of wave functions reflected at the two interfaces of a layer. In the lowest approximation with respect to F in expressions (25) and (26), one obtains for the position E_n^l of the nth peak

$$E_n^l = 2n\pi^2 \frac{\hbar^2}{m^* d_W^2} \ , \tag{29}$$

and for the corresponding period

$$\Delta_n^l = \pi \frac{\hbar}{\sqrt{2m^*} d_W} \sqrt{E_n^l} \ . \tag{30}$$

This implies that, for low fields, the oscillation period and, hence, the bandwidth, does not depend on the electric field (Fig. 11).

The arguments of the g_i and h_j in Eq. (24) refer to well and barrier regions, respectively. If i and j are taken for adjacent layers, the g_i and h_j may be combined into one expression with an argument $(\gamma_i - \delta_{i+2})$ referring to a whole SL period. For not-too-small N, the product of the thus-obtained expressions approximates the N-fold product of the g_i and h_j in (24) very well. Since the arguments of the approximate expression vary only slightly with i, one can substitute the N-fold product by one expression to the Nth power. The latter can be expressed in terms of trigonometric functions with shorter periods, e.g., $\cos^N(kd) = \cos(Nkd) + \ldots$. This explains why the number of "long-period" oscillations per band equals the number of periods N. Investigating the periodicity due to

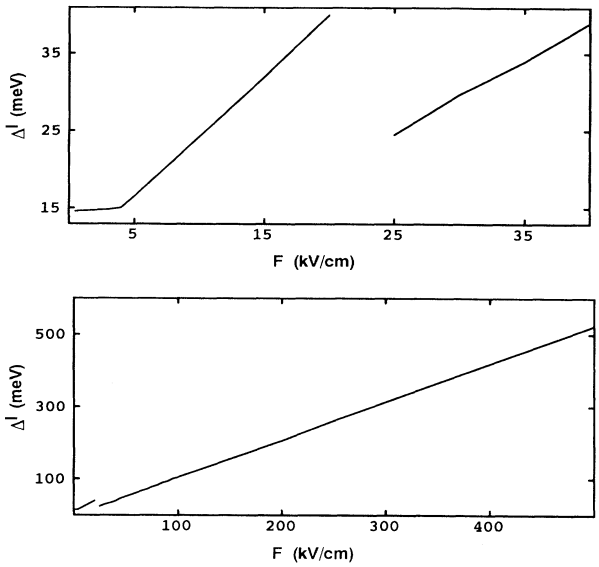

FIG. 13. Spacing Δ^l of "long-period" (WS) peaks as a function of field F of SL3 at $E = 2.5$ eV.

the "long-period" oscillations of SL3 yields a SL period d of ≈ 100 Å, coinciding very well with $d = d_W + d_B = 102$ Å. If the field strength can no longer be considered to be low, Δ_n^l starts to depend on F. Numerical results are shown in Fig. 13. Up to field strengths of about 5×10^3 V/cm, Δ_n^l remains constant, in agreement with the low-field approximation (30). Then Δ_n^l rises with F monotonously up to 2–2.5×10^4 V/cm. Increasing the field strength further, any "long-period" oscillation splits into two at a certain critical value, changing the period to $eF(d_W + d_B)$. From this field strength on, the "long-period" oscillations behave similarly to the WS ladder in the below-barrier region. For fields greater than 5×10^5 V/cm, the "long-period" peaks vanish [Fig. 11(d)]. This resembles the occurrence and disappearance of the Wannier-Stark ladder below barriers. If eFd exceeds several long periods for zero electric field, the "long-period" peaks with period eFd occur. If the field is increased further, $\hbar\theta$ becomes greater than the band gap, which is about 150–200 meV, and interband tunneling becomes possible. Then the "long-period" peaks disappear. In spite of their similarity with WS peaks below the barriers, the "long-period" peaks may not be traced back to WS localization [Fig. 8(c)], as this may be done below the barriers. The wave functions for "long-period"-peak energies remain delocalized in the whole range of field strengths.

IV. CONCLUSIONS

We have examined the effects of external electric fields on the DOS of various finite SL structures embedded within two infinitely extending barriers. The DOS spectra give clear evidence for the existence of WS localization in the below-barrier region. The existence of a WS

ladder depends on the field. It occurs only in a certain field range which depends on the actual parameters of the heterostructure. The states forming a WS ladder at higher fields evolve from the zero-field bound states. The level separation for the WS localization to occur amounts to a certain portion of the zero-field bandwidth (rather than the whole). For moderate and high fields, states from above the barriers are pushed downwards into the Stark ladder region. They form the "above-barrier" states, whose peaks are less pronounced and broader than those stemming from the WS levels.

The DOS in the spectral region above the barrier is characterized by "short-period" oscillations with a superimposed "long-period" oscillation. The "short-period" oscillations behave similar to Franz-Keldysh oscillations, whereas the "long-period" oscillations resemble a WS-like behavior in a certain field range, although no WS localization is observed above the barriers. Similar results are obtained for SL's embedded within two wells instead of barriers.

[1]G. Bastard, E. E. Mendez, L. L. Chang, and L. Esaki, Phys. Rev. B **28**, 3241 (1983).
[2]E. J. Austin and M. Jaros, Phys. Rev. B **31**, 5569 (1985).
[3]D. A. B. Miller, D. S. Chemla, T. C. Amen, A. C. Gossard, W. Wiegmann, T. H. Wood, and C. A. Burges, Phys. Rev. B **32**, 1043 (1985).
[4]E. J. Austin and M. Jaros, J. Appl. Phys. **62**, 558 (1987).
[5]K. Bajema, R. Merlin, F.-Y. Juang, S.-C. Hong, J. Singh, and P. K. Bhattacharya, Phys. Rev. B **36**, 1300 (1987).
[6]L. A. Cury and N. Stuart, Superlatt. Microstruct. **3**, 175 (1987).
[7]J. Bleuse, P. Voisin, M. Allovon, and M. Quillec, Appl. Phys. Lett. **53**, 2632 (1988).
[8]E. E. Mendez, F. Agulló-Rueda, J. M. Hong, and L. L. Chang, in *Proceedings of the 19th International Conference on the Physics of Semiconductors,* edited by W. Zawadzki (Warsaw, Poland, 1988), p. 415.
[9]E. E. Mendez, F. Agulló-Rueda, and J. M. Hong, Phys. Rev. Lett. **60**, 2426 (1988).
[10]R. Enderlein, T. Holz, and J. L. Gondar, Phys. Status Solidi B **156**, 259 (1989).
[11]R. H. Yan, F. Laruelle, and L. A. Coldren, Appl. Phys. Lett. **55**, 2002 (1989).
[12]F. Cerdeira *et al.*, Phys. Rev. B **42**, 9480 (1990).
[13]J. P. Hagon and M. Jaros, Phys. Rev. B **41**, 2900 (1990).
[14]R. P. Leavitt and J. W. Little, Phys. Rev. B **41**, 5174 (1990).
[15]R. P. Leavitt and J. W. Little, Phys. Rev. B **42**, 11 784 (1990).
[16]E. E. Mendez, F. Agulló-Rueda, and J. M. Hong, Appl. Phys. Lett. **56**, 2545 (1990).
[17]D. A. Broido, Superlatt. Microstruct. **3**, 13 (1987).
[18]K. Satzke, G. Weiser, W. Stolz, and K. Ploog, Phys. Rev. B **43**, 2263 (1991).
[19]P. Voisin, J. Bleuse, C. Bonde, S. Gaillard, C. Alibert, and A. Regrency, Phys. Rev. Lett. **61**, 1639 (1988).
[20]F. Pollak, Superlatt. Microstruct. **10**, 333 (1991).
[21]W. Trzeciakowski and M. Gurioli, Phys. Rev. B **44**, 3880 (1991).
[22]K. H. Schmidt, A. D'Intino, N. Linder, M. Tuna, G. H. Döhler, H. T. Grahn, K. Ploog, K. Kawashima, and K. Fujiwara, Superlatt. Microstruct. **12**, 181 (1992).
[23]K. Leo, J. Feldmann, J. Shah, G. von Plessen, P. Thomas, S. Schmitt-Rink, and J. Cunningham, Superlatt. Microstruct. **13**, 55 (1993).
[24]W. Franz, Z. Naturforsch. Teil A **13**, 484 (1958).
[25]L. V. Keldysh, Zh. Eksp. Teor. Fiz. **34**, 1138 (1958).
[26]G. H. Wannier, Phys. Rev. **117**, 432 (1960).
[27]R. Enderlein, Phys. Rev. B **42**, 4708 (1990).
[28]H. A. Antosiewicz, in *Handbook of Mathematical Functions,* edited by M. Abramowitz and I. A. Stegun (Dover, New York, 1964).